



# Analysis of Optimal Gain of MPSK Signal Based on BSR

ZhiChong Shen<sup>(✉)</sup>, JinQuan Ma, Di Yang, and XiaoLong Shen

Information System Engineering College, Information Engineering University,  
ZhengZhou, China

**Abstract.** Bistable Stochastic Resonance (BSR) system is a nonlinear system. When the noise variance of the noisy periodic signal has a certain relationship with the signal, after the noisy signal passes through the system, the noise energy can be partially converted to the signal energy, thus providing a means of signal enhancement. Later, with the introduction of the Aperiodic Stochastic Resonance (ASR) system theory, the stochastic resonance theory can be applied to the field of communication. At present, the most application of stochastic resonance in communication is in binary modulation signal area. This paper will be discussing the enhanced effect of stochastic resonance on the multi-ary phase modulation signal, deriving the expression of the MPSK signal power after resonance, and proving that the signal power spectral density after stochastic resonance has no effect on phase. Defining the signal-to-noise ratio's gain and amplitude's gain, and giving the range of the gain and the maximum value of the gain that stochastic resonance can improve the signal-to-noise ratio when the signal carrier amplitude and signal carrier frequency are determined.

**Keywords:** Stochastic resonance · Signal processing · Bistable system

## 1 Introduction

As one of the commonly used digital modulation signals, the phase modulation signal has always been widely concerned in the communication field. In recent years, attention to detecting PSK signals has begun to enter the field of low signal-to-noise ratio. As a method of using noise energy to achieve signal enhancement, stochastic resonance has naturally attracted widespread attention [1, 2]. In 2014, Liu Jin studied the enhancement effect of stochastic resonance on the BPAM signal and gave the corresponding enhancement model [3]. In the same year, Liu Jin again extended the enhancement model to FSK signals [4], and again in 2015 to MPAM signals [5]. In 2018, Zhang Zheng proposed a PSK signal symbol rate estimation method based on stochastic resonance [6]. The following year, Zhang Zheng introduced an artificial fish swarm algorithm to realize the application of stochastic resonance in the detection of a variety of digital modulation signals [7]. In the same year, Linlin Liang et al. studied the

application of stochastic resonance in 4PAM signal detection [8]. However, for MPSK signals, the discussion of stochastic resonance is mainly concentrated in the field of computer algorithms, and there are still few discussions on theoretical models.

In order to explore the common points of different types of PSK signals after stochastic resonance, this paper takes the signal power as the starting point, and through derivation, gives the expression of the power spectral density of the MPSK signal after the stochastic resonance of the bistable system, and proves the PSK signal The phase change of  $\phi$  will not affect the power spectral density, thus simplifying the influence of stochastic resonance on the signal. Then, define the signal-to-noise ratio gain and give its expression, calculate the range of the signal-to-noise ratio when stochastic resonance obtains the gain, and prove that there is a maximum gain, which provides an idea for processing unknown low-signal-to-noise ratio signals.

## 2 MPSK Parameter Calculation Based on Bistable System

### 2.1 Power Spectral Density

Suppose the model of the signal is  $s(t) = Ag_t(t) \cos(2\pi f_c t + 2\pi(m - 1)/M)$ , where  $A$  is the signal amplitude,  $g_t(t)$  is the signal pulse shape,  $f_c$  is the signal carrier frequency,  $2\pi(m - 1)/M$  is the  $M$  phases of the signal. The probability that the output signal of the bistable system will transition to the steady-state point of the signal at time  $t$  is respectively  $m_{\pm}(t)$ . and the probability within the two potential wells satisfies

$$m_+(t) = 1 - m_-(t) = \int_{x_0}^{+\infty} p(x)dx \tag{1}$$

Considering the driving force of the periodic signal, due to the periodic driving of the periodic signal, the transfer rate  $R_{\pm}(t)$  of the bistable system output signal between the discrete steady states of the two potential wells is also periodic in time, and satisfies The relationship is as follows:

$$\frac{dm_+(t)}{dt} = -\frac{dm_-(t)}{dt} = R_-(t) - [R_+(t) + R_-(t)] m_+(t) \tag{2}$$

The solution to linear first-order differential equation (2) is given by:

$$\begin{cases} m_+(t) = g^{-1}(t)m_+(t_0)g(t_0) + g^{-1}(t) \int_{t_0}^t R_-(\tau)g(\tau)d\tau \\ g(t) = e^{\int_{t_0}^t [R_+(\tau)+R_-(\tau)]d\tau} \end{cases} \tag{3}$$

Assume that  $R_{\pm}(t) = f(\lambda \pm \varphi_0 \cos(\omega_c t + 2\pi(m - 1)/M))$  Where  $f$  is an exponential function,  $\lambda, \varphi_0$  are dimensionless constants,  $\omega_c = 2\pi/T = 2\pi f_c, M = 2^k$ ,

$k \in N^+$ ,  $m = \{1, 2, \dots, M\}$ . Although  $\varphi_0 \cos(\omega_c t + 2\pi(m - 1)/M)$  have discontinuous points in  $(-\infty, \infty)$ , it is a continuous function in one period. So we can use Taylor expansion for  $R_{\pm}(t)$  in one period, then we have

$$R_{\pm}(t) = \frac{1}{2}(\alpha_0 \mp \alpha_1 \varphi_0 \cos(\omega_c t + \theta) + \alpha_1 \varphi_0^2 \cos^2(\omega_c t + \theta) \mp \dots) \tag{4}$$

$$R_+(t) + R_-(t) = \alpha_0 + \alpha_1 \varphi_0^2 \cos^2(\omega_c t + \theta) + \dots \tag{5}$$

where  $\frac{1}{2}\alpha_0 = f(\lambda)$ ,  $\frac{1}{2}\alpha_n = \frac{(-1)^n}{n!} \left(\frac{d}{d\varphi}\right)^n f(\lambda)$ . Substituting Eqs. (4) and (5) into Eq. (3), the asymptotic analytical solution of the probability  $m_+(t)$  that the output signal of the system is in the steady-state position of the potential well is obtained:

$$m_+(t|x_0, t_0) = \frac{1}{2}e^{-\alpha_0(t-t_0)} \left( 2\delta_{x_0c} - 1 - \frac{\alpha_1 \varphi_0 \cos(\omega_c t + \theta - \phi)}{\sqrt{\alpha_0^2 + \omega_c^2}} \right) + \frac{1}{2} \left( 1 + \frac{\alpha_1 \varphi_0 \cos(\omega_c t + \theta - \phi)}{\sqrt{\alpha_0^2 + \omega_c^2}} \right) \tag{6}$$

where  $\phi = \arctan \frac{\omega_c}{\alpha_0}$ ,  $\delta_{x_0c} = \begin{cases} 1, c = +\sqrt{a/b} \\ 0, c = -\sqrt{a/b} \end{cases}$ .

According to Eq. (6), it can be calculated:

$$\langle x(t)x(t + \tau) \rangle = c^2 e^{-\alpha_0|\tau|} \left( 1 - \frac{\alpha_1^2 \varphi_0^2 \cos^2(\omega_c t + \theta - \phi)}{\alpha_0^2 + \omega_c^2} \right) + \frac{c^2 \alpha_1^2 \varphi_0^2 \{ \cos(\omega_c \tau) + \cos^2[\omega_c(2t + 2\theta + \tau) + 2\phi] \}}{2(\alpha_0^2 + \omega_c^2)} \tag{7}$$

Further calculations to get the average autocorrelation:

$$\begin{aligned} & \langle \langle x(t)x(t + \tau) \rangle \rangle_t \\ &= \frac{\omega_c}{2\pi} \int_0^{\frac{2\pi}{\omega_c}} \left[ c^2 e^{-\alpha_0|\tau|} \left( 1 - \frac{\alpha_1^2 \varphi_0^2 \cos^2(\omega_c t + \theta - \phi)}{\alpha_0^2 + \omega_c^2} \right) + \frac{c^2 \alpha_1^2 \varphi_0^2 \{ \cos(\omega_c \tau) + \cos^2[\omega_c(2t + 2\theta + \tau) + 2\phi] \}}{2(\alpha_0^2 + \omega_c^2)} \right] dt \\ &= \frac{\omega_c}{2\pi} \int_0^{\frac{2\pi}{\omega_c}} [f_1(t) + f_2(t) + f_3(t)] dt \end{aligned} \tag{8}$$

where

$$f_1(t) = c^2 e^{-\alpha_0|\tau|} + \frac{c^2 \alpha_1^2 \varphi_0^2 \cos(\omega_c \tau)}{2(\alpha_0^2 + \omega_c^2)} \tag{9}$$

$$f_2(t) = \frac{c^2 e^{-\alpha_0|\tau|} \alpha_1^2 \varphi_0^2 \cos^2(\omega_c t + \theta - \phi)}{\alpha_0^2 + \omega_c^2} \tag{10}$$

$$f_3(t) = \frac{c^2 \alpha_1^2 \varphi_0^2 \cos^2[\omega_c(2t + 2\theta + \tau) + 2\phi]}{2(\alpha_0^2 + \omega_c^2)} \tag{11}$$

Because of

$$\begin{aligned} & \frac{\omega_c}{2\pi} \int_0^{\frac{2\pi}{\omega_c}} f_2(t) dt \\ &= \frac{\omega_c}{2\pi} \int_0^{\frac{2\pi}{\omega_c}} \frac{c^2 e^{-\alpha_0|\tau|} \alpha_1^2 \varphi_0^2 \cos^2(\omega_c t + \theta - \phi)}{\alpha_0^2 + \omega_c^2} dt \\ &= -\frac{\omega_c c^2 e^{-\alpha_0|\tau|} \alpha_1^2 \varphi_0^2}{2\pi(\alpha_0^2 + \omega_c^2)} \left( \frac{t + \theta - \phi}{2} + \frac{\sin[2(\omega_c t + \theta - \phi)]}{4\omega_c} \right) \Bigg|_0^{\frac{2\pi}{\omega_c}} \\ &= -\frac{c^2 e^{-\alpha_0|\tau|} \alpha_1^2 \varphi_0^2}{2(\alpha_0^2 + \omega_c^2)} \end{aligned} \tag{12}$$

$$\begin{aligned}
 & \frac{\omega_c}{2\pi} \int_0^{\frac{2\pi}{\omega_c}} f_3(t) dt \\
 &= \frac{\omega_c}{2\pi} \int_0^{\frac{2\pi}{\omega_c}} \frac{c^2 \alpha_1^2 \varphi_0^2 \cos^2[\omega_c(2t+2\theta+\tau)+2\phi]}{2(\alpha_0^2+\omega_c^2)} dt \\
 &= \frac{c^2 \alpha_1^2 \varphi_0^2 \cos[\omega_c(2t+2\theta+\tau)+2\phi]}{8\pi(\alpha_0^2+\omega_c^2)} \Bigg|_0^{\frac{2\pi}{\omega_c}} = 0
 \end{aligned} \tag{13}$$

so

$$\begin{aligned}
 & \langle\langle x(t)x(t+\tau) \rangle\rangle_t \\
 &= \frac{\omega_c}{2\pi} \int_0^{\frac{2\pi}{\omega_c}} [f_1(t) + f_2(t) + f_3(t)] dt \\
 &= c^2 e^{-\alpha_0|\tau|} \left( 1 - \frac{\alpha_1^2 \varphi_0^2}{2(\alpha_0^2+\omega_c^2)} \right) + \frac{c^2 \alpha_1^2 \varphi_0^2 \cos(\omega_c \tau)}{2(\alpha_0^2+\omega_c^2)}
 \end{aligned} \tag{14}$$

From Eq. (14), we can get the bilateral power spectral density of the output signal:

$$\begin{aligned}
 \langle S(\omega) \rangle_t &= \int_{-\infty}^{+\infty} \langle\langle x(t)x(t+\tau) \rangle\rangle_t e^{-j\omega\tau} d\tau \\
 &= \left( 1 - \frac{\alpha_1^2 \varphi_0^2}{2(\alpha_0^2+\omega_c^2)} \right) \left( \frac{2c^2 \alpha_0}{\alpha_0^2+\omega_c^2} \right) + \frac{\pi c^2 \alpha_1^2 \varphi_0^2}{2(\alpha_0^2+\omega_c^2)} [\delta(\omega - \omega_c) + \delta(\omega + \omega_c)]
 \end{aligned} \tag{15}$$

Then the unilateral power spectral density is:

$$S(\omega) = \left( 1 - \frac{\alpha_1^2 \varphi_0^2}{2(\alpha_0^2 + \omega_c^2)} \right) \left( \frac{4c^2 \alpha_0}{\alpha_0^2 + \omega_c^2} \right) + \frac{\pi c^2 \alpha_1^2 \varphi_0^2}{\alpha_0^2 + \omega_c^2} \delta(\omega - \omega_c) \tag{16}$$

Where the signal component is  $S_s(\omega) = \frac{\pi c^2 \alpha_1^2 \varphi_0^2}{\alpha_0^2 + \omega_c^2} \delta(\omega - \omega_c)$ , the noise component is  $S_n(\omega) = \left( 1 - \frac{\alpha_1^2 \varphi_0^2}{2(\alpha_0^2 + \omega_c^2)} \right) \left( \frac{4c^2 \alpha_0}{\alpha_0^2 + \omega_c^2} \right)$ .

It can be seen from Eq. (6) and (16) that the change of the phase component  $\theta$  in  $R_{\pm}(t)$  has no effect on the power spectral density  $S(\omega)$ , so the expressions for any  $\theta$  and  $S(\omega)$  remain unchanged, means that for any MPSK signal, the signal power spectrum expression is unique.

### 2.2 Gain of Signal-to-Noise Ratio

The bistable system model can be expressed as  $\frac{dx}{dt} = ax + bx^3 + A \cos(\omega_c t + \theta) + \sqrt{D}n(t)$ , where  $n(t)$  is AWGN and satisfied  $\langle n(t) \rangle = 0$ ,  $\langle n(t)n(t+\tau) \rangle = \delta(\tau)$ ,  $D$  is the variance. According to the literature [1], Eq. (10) can be calculated as:

$$S(\omega) = \left( 1 - \frac{4a^3 A^2 e^{-\frac{a^2}{bD}}}{b\pi^2 D^2 + \omega_c^2} \right) \left( \frac{4\sqrt{2}a^2 e^{-\frac{a^2}{2bD}}}{\frac{2a^2}{\pi^2} e^{-\frac{a^2}{bD}} + \omega^2} \right) + \left( \frac{8a^4 A^2 e^{-\frac{a^2}{bD}}}{b^2 \pi D^2 + \omega_c^2} \right) \delta(\omega - \omega_c) \tag{17}$$

Where

$$S_s(\omega) = \left( \frac{8a^4 A^2 e^{-\frac{a^2}{bD}}}{b^2 \pi D^2 + \omega_c^2} \right) \delta(\omega - \omega_c) \tag{18}$$

and

$$S_n(\omega) = \left( 1 - \frac{4a^3 A^2 e^{-\frac{a^2}{bD}}}{b\pi^2 D^2 + \omega_c^2} \right) \left( \frac{4\sqrt{2}a^2 e^{-\frac{a^2}{2bD}}}{\frac{2a^2}{\pi^2} e^{-\frac{a^2}{bD}} + \omega^2} \right) \tag{19}$$

Obviously  $S_s(\omega) > 0$  and  $S_n(\omega) > 0$ , so  $1 - \frac{\frac{4a^3A^2}{b\pi^2D^2}e^{-\frac{a^2}{bD}}}{\frac{2a^2}{\pi^2}e^{-\frac{a^2}{bD}} + \omega_c^2} > 0$ , substitute  $\omega_c = 2\pi f_c$  to get:

$$f_c > \frac{a}{\sqrt{2\pi^2}} e^{-\frac{a^2}{2bD}} \sqrt{\frac{2aA^2}{bD^2} - 1} \tag{20}$$

Therefore, when the signal carrier frequency  $f_c$  meets the conditions described in Eq. (20), the input signal can trigger stochastic resonance.

According to Eq. (17), the average power of the signal after system enhancement can be obtained as:

$$P_{S_s(\omega),out} = \frac{1}{2\pi} \int_0^{+\infty} S_s(\omega) d\omega = \frac{\frac{4a^4A^2}{b^2\pi^2D^2}e^{-\frac{a^2}{bD}}}{\frac{2a^2}{\pi^2}e^{-\frac{a^2}{bD}} + \omega_c^2} \tag{21}$$

$$P_{S_n(\omega),out} = \frac{1}{2\pi} \int_0^{+\infty} S_\xi(\omega) d\omega = \frac{a}{b} - \frac{\frac{4a^4A^2}{b^2\pi^2D^2}e^{-\frac{a^2}{bD}}}{\frac{2a^2}{\pi^2}e^{-\frac{a^2}{bD}} + \omega_c^2} \tag{22}$$

Then the output signal-to-noise ratio is:

$$SNR_{out} = 10 \lg \frac{P_{S_s(\omega),out}}{P_{S_\xi(\omega),out}} = 10 \lg \frac{\frac{4a^3A^2}{b\pi^2D^2}e^{-\frac{a^2}{bD}}}{\frac{2a^2}{\pi^2}e^{-\frac{a^2}{bD}} \left(1 - \frac{2aA^2}{bD^2}\right) + \omega_c^2} \tag{23}$$

Define the signal-to-noise ratio gain  $Gain = SNR_{out} - SNR_{in}$ , from the MPSK signal model we know that the input signal-to-noise ratio is  $SNR_{in} = 10 \lg \frac{A^2}{2D}$ , then we have

$$Gain = 10 \lg \frac{\frac{8a^3}{b\pi^2D}e^{-\frac{a^2}{bD}}}{\frac{2a^2}{\pi^2}e^{-\frac{a^2}{bD}} \left(1 - \frac{2aA^2}{bD^2}\right) + \omega_c^2} = 10 \lg G \tag{24}$$

When  $G > 1$ , we have

$$\frac{2a^2}{b\pi^2} (4aD - bD^2 + 2aA^2) - \omega_c^2 D^2 e^{\frac{a^2}{bD}} = G_1 - G_2 > 0 \tag{25}$$

Notice that  $\frac{\partial G_2}{\partial D} = \omega_c^2 (2D - \frac{a^2}{b}) e^{\frac{a^2}{bD}}$ , when  $\frac{\partial G_2}{\partial D} = 0$  we have  $D = \frac{a^2}{2b}$ , then  $G_2 = \frac{a^4 \omega_c^2 e^2}{4b^2}$ .

When  $D > \frac{a^2}{2b}$ , expand  $\omega_c^2 D^2 e^{\frac{a^2}{bD}}$  to  $\omega_c^2 D^2 (1 + \frac{a^2}{bD} + \frac{a^4}{2b^2 D^2})$ , the formula (25) is transformed into

$$\frac{2a^2}{b\pi^2} (4aD - bD^2 + 2aA^2) - \omega_c^2 D^2 (1 + \frac{a^2}{bD} + \frac{a^4}{2b^2 D^2}) > 0 \tag{26}$$

then

$$D < \frac{\frac{8a^3}{b} - \frac{a^2\pi^2\omega_c^2}{b} + \pi^2 \sqrt{\left(\frac{8a^3}{b\pi^2} - \frac{a^2\omega_c^2}{b}\right)^2 + 4\left(\frac{2a^2}{\pi^2} + \omega_c^2\right)\left(\frac{4a^3A^2}{b\pi^2} - \frac{1}{2}a^4b^2\omega_c^2\right)}}{2(2a^2 + \pi^2\omega_c^2)} = D_{\max} \quad (27)$$

When  $0 < D < \frac{a^2}{2b}$ , multiply both sides of formula (25) by  $D^2$  and expand  $\omega_c^2 D^2 e^{\frac{a^2}{bD}}$  to  $\omega_c^2 D^2 (1 + \frac{a^2}{bD} + \frac{a^4}{2b^2 D^2} + \frac{a^6}{6b^3 D^3} + \frac{a^8}{24b^4 D^4})$ , the formula (25) is transformed into

$$\frac{2a^2}{b\pi^2} D^2 (4aD - bD^2 + 2aA^2) - \omega_c^2 D^4 \left(1 + \frac{a^2}{bD} + \frac{a^4}{2b^2 D^2} + \frac{a^6}{6b^3 D^3} + \frac{a^8}{24b^4 D^4}\right) > 0 \quad (28)$$

then  $D_{\min}$  can be calculated.

Finally we get the variance range when stochastic resonance has positive gain, and the signal-to-noise ratio range of the input signal is

$$10 \lg \frac{A^2}{2D_{\max}} < SNR_{in} < 10 \lg \frac{A^2}{2D_{\min}} \quad (29)$$

When the signal-to-noise ratio of the input signal is within the range described in formula (29), stochastic resonance can achieve the effect of enhancing the signal.

### 3 Simulations

#### 3.1 Amplitude Enhancement Effect

First, we observe the signal waveform when the signal-to-noise ratio is different when the amplitude and carrier frequency of the input signal are constant. Verify that when the signal amplitude and signal carrier frequency are determined, when the signal-to-noise ratio is within a given range, stochastic resonance can produce an amplitude enhancement effect.

Take the QPSK signal as an example, set the bistable parameters as  $a = 1$ ,  $b = 1$ , and the signal amplitude  $A = 0.5$ . Then, when the signal-to-noise ratio gain is greater than 1, the noise variance can be solved by Eqs. (27) and (28) and the range is  $0.1543 < D < 2.9022$ , so the input signal SNR range is  $-13.6582 \text{ dB} < SNR_{in} < -0.9146 \text{ dB}$ . Set the signal-to-noise ratio  $SNR_{in} = -5 \text{ dB}$ , and the noise variance is 0.3953, which meets the requirements. Set the signal carrier frequency  $f_c = 0.0318 \text{ Hz}$ , then  $f_c > 0.03 \text{ Hz}$  conforms to the range described in formula (20). Number of symbols  $N = 5$ , symbol rate  $R_s = 0.01 \text{ bps}$ .

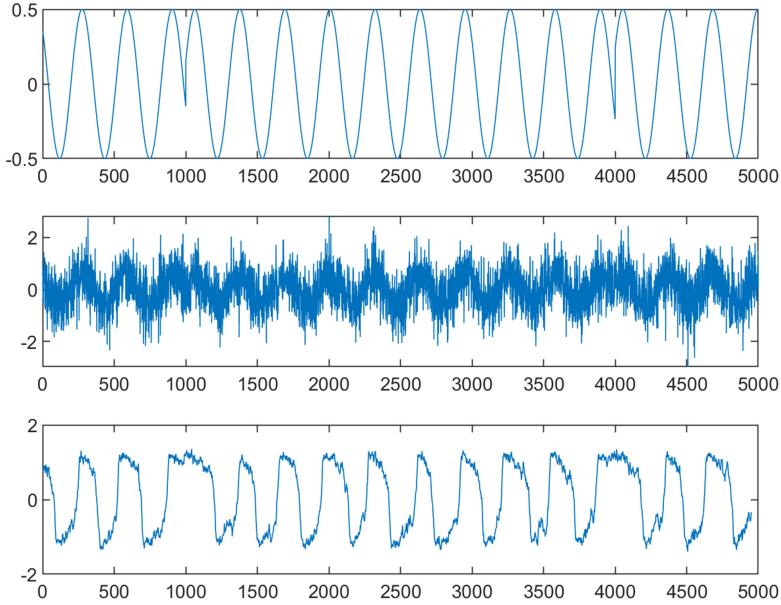


**Fig. 1.** QPSK signal waveform before and after stochastic resonance

As shown in Fig. 1, the first column of Fig. 1 is the noise-free QPSK signal waveform, the second column is the noise-added QPSK signal waveform, and the third column is the QPSK signal waveform after resonance.

According to formula (18), we can assume that the unilateral power spectral density of a certain signal  $s_h(t)$  is equal to formula (18), then

$$s_h(t) = \frac{\frac{2\sqrt{2}a^2 A}{b\pi D} e^{-\frac{a^2}{2bD}}}{\sqrt{\frac{2a^2}{\pi^2} e^{-\frac{a^2}{bD}} + \omega_c^2}} \cos(\omega_c t + \theta) \tag{30}$$

can be obtained, and the amplitude gain is defined as

$$G_{Amplitude} = \frac{A_{s_h}}{A_{s_s}} = \frac{\frac{2\sqrt{2}a^2}{b\pi D} e^{-\frac{a^2}{2bD}}}{\sqrt{\frac{2a^2}{\pi^2} e^{-\frac{a^2}{bD}} + \omega_c^2}} \tag{31}$$

according to the aforementioned QPSK signal parameters, we can calculate  $G_{Amplitude} = 2.2828$ , which is consistent with the experimental results. It shows that after stochastic resonance, noise energy is successfully converted into signal energy, which shows the effectiveness of stochastic resonance.

Similarly, for 8PSK signals, set the signal-to-noise ratio  $SNR_{in} = -5$  dB and the signal carrier frequency  $f_c = 0.0318$  Hz. Number of symbols  $N = 10$ , symbol rate  $R_s = 0.01$  bps (Fig. 2).

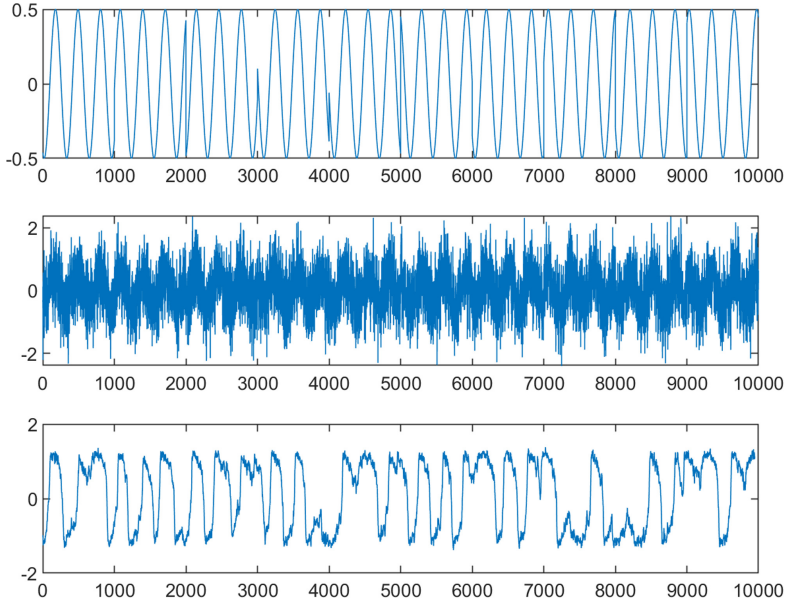


**Fig. 2.** 8PSK signal waveform before and after stochastic resonance

It can be seen that after stochastic resonance, for QPSK and 8PSK signals, the noise energy is successfully transferred to the signal energy, which illustrates the effectiveness of stochastic resonance for MPSK signals.

**3.2 Signal-to-Noise Ratio Gain Curve**

Now we examine the signal-to-noise ratio and signal-to-noise ratio gain of the output signal when the signal-to-noise ratio of the input signal changes.

Take the QPSK signal as an example, set the variance  $D$  from 0.1 to 1.3, the signal carrier frequency  $f_c = 0.04$  Hz, and the other parameters remain unchanged.

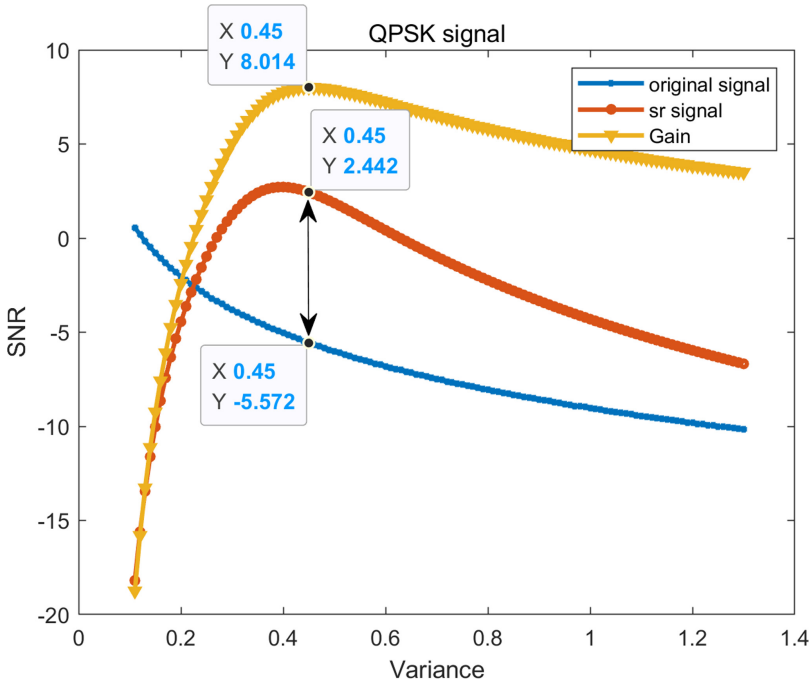


**Fig. 3.** Input, output signal-to-noise ratio and gain curve of QPSK signal

It can be seen from Fig. 3 that when the variance  $D = 0.45$ , the difference of the signal-to-noise ratio before and after the signal resonance is the largest, which is 8.0140 dB. System parameters, signal amplitude and carrier frequency, signal-to-noise ratio gain have maximum values.

For different PSK signals, observe the changes in the signal-to-noise ratio before and after the signal resonance when the variance changes. Set the BPSK, QPSK, and 8PSK signals with the same signal parameters. The parameters are: the number of symbols  $N = 500$ , the signal amplitude  $A = 0.5$ , the carrier frequency  $f_c = 0.04$  Hz, and the symbol rate  $R_s = 0.01$  bps. Set the input signal-to-noise ratio  $SNR_{in}$  to increase from  $-12$  dB to  $0$  dB, perform 500 Monte Carlo experiments and take the average value of the signal-to-noise ratio gain. The experimental results are as Fig. 4 follows.

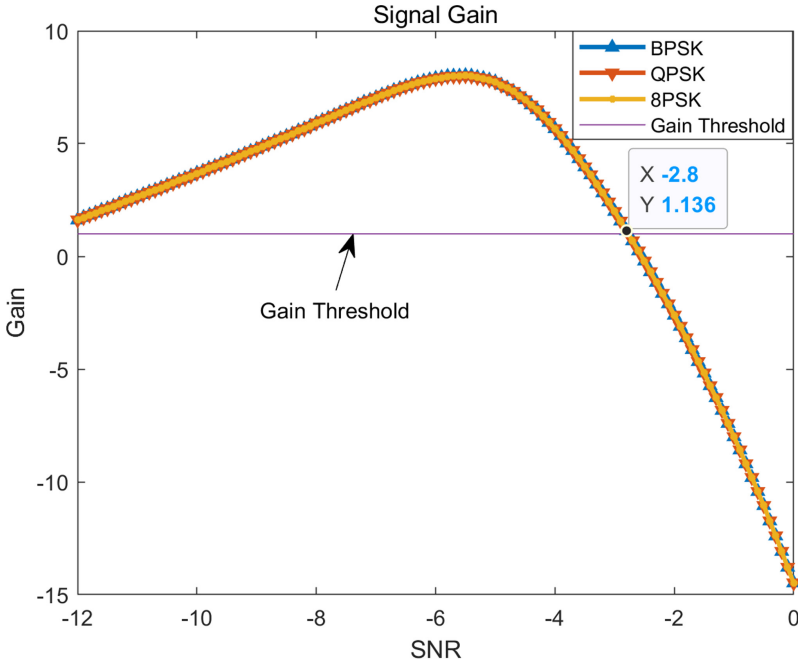


**Fig. 4.** BPSK, QPSK, 8PSK signal-to-noise ratio gain curve

As shown in Fig. 4, the purple solid line is the gain threshold  $G = 1$ . When  $G > 1$ ,  $SNR_{out} - SNR_{in} > 0$ , that is, the output signal-to-noise ratio is higher than the input signal-to-noise ratio. At this time, resonance can enhance the effect. When  $SNR_{in} > -2.7$  dB, the gain  $G > 1$ , and the noise variance  $D \approx 0.2$ , which means that when the variance  $D > 0.2$ , stochastic resonance can enhance the effect, and when the signal amplitude is the same as the signal carrier frequency, the gain of different MPSK signals is the same. It shows that the enhancement effect of stochastic resonance has nothing to do with the change of signal phase.

## 4 Conclusions

Based on the adiabatic approximation theory, starting from the expression of the bistable system, this paper proves through calculation that the signal phase change will not affect the signal power spectral density of the noisy signal after stochastic resonance. It shows that the MPSK signal has the stochastic resonance of the bistable system. Uniform power spectrum density, and the correctness of the conclusion is verified by simulation experiment. When the signal amplitude and carrier frequency are determined, within a certain range, stochastic resonance can enhance MPSK, and there is a maximum gain related to the amplitude

and the carrier frequency. It provides a new idea for the application of stochastic resonance in signal processing.

## References

1. Mcnamara, B., Wiesenfeld, K.: Theory of stochastic resonance. *Phys. Rev. A Gen. Phys.* **39**(9), 4854–4869 (1989)
2. Collins, J.J.: Aperiodic stochastic resonance in excitable systems. *Phys. Rev. E Stat. Phys. Plasmas Fluids Rel. Interdisc. Top.* **52**(4), R3321 (1995)
3. Liu, J., Li, Z., Guan, L., Pan, L.: A novel parameter-tuned stochastic resonator for binary PAM signal processing at low SNR. *IEEE Commun. Lett.* **18**(3), 427–430 (2014). <https://doi.org/10.1109/LCOMM.2014.011214.132465>
4. Liu, J., Li, Z., Gao, R., Bo, J., Guan, L.: A Novel detector based on parameter-induced bistable stochastic resonance for FSK signal processing at low SNR. In: 2014 IEEE International Conference on Computer and Information Technology, Xi'an, China, pp. 832–836 (2014). <https://doi.org/10.1109/CIT.2014.127>
5. Liu, J., Li, Z., Gao, R., Bai, J., Liang, L.: Multi-ary pulse amplitude modulated signal processing using bistable stochastic resonance. In: 2015 International Conference on Noise and Fluctuations (ICNF), Xi'an, China, pp. 1–4 (2015). <https://doi.org/10.1109/ICNF.2015.7288557>
6. Zhang, Z., Ma, J., et al.: A PSK signal symbol rate estimation algorithm based on the combination of stochastic resonance and wavelet transform. *IOP Conf. Ser. Mater. Sci. Eng.* **449** (2018)
7. Zhang, Z., Ma, J.: Adaptive parameter-tuning stochastic resonance based on SVD and its application in weak IF digital signal enhancement. *J. Adv. Signal Process.* **2019**(1) (2019)
8. Liang, L., Zhang, N., Huang, H., Li, Z.: Bistable stochastic resonance enhanced 4-ary PAM signal detection under low SNR. *China Commun.* **16**(4), 196–207 (2019). <https://doi.org/10.12676/j.cc.2019.04.015>